

A Multimodal Approach for Fluid Overload Prediction: Integrating Lung Ultrasound and Clinical Data

Tianqi Yang¹, Nantheera Anantrasirichai¹, Oktay Karakus², Marco Allinovi³, and Alin Achim¹

¹*Visual Information Lab, University of Bristol, Bristol, UK*

²*School of Computer Science and Informatics, Cardiff University, Cardiff, UK*

³*Nephrology, Dialysis and Transplantation, Careggi University Hospital, Florence, Italy*

Abstract—Managing fluid balance in dialysis patients is crucial, as improper management can lead to severe complications. In this paper, we propose a multimodal approach that integrates visual features from lung ultrasound images with clinical data to enhance the prediction of excess body fluid. Our framework employs independent encoders to extract features for each modality and combines them through a cross-domain attention mechanism to capture complementary information. By framing the prediction as a classification task, the model achieves significantly better performance than regression. The results demonstrate that multimodal models consistently outperform single-modality models, particularly when attention mechanisms prioritize tabular data. Pseudo-sample generation further contributes to mitigating the imbalanced classification problem, achieving the highest accuracy of 88.31%. This study underscores the effectiveness of multimodal learning for fluid overload management in dialysis patients, offering valuable insights for improved clinical outcomes.

Index Terms—Multimodal, imbalanced classification, lung ultrasound, hypervolemia, dialysis

I. INTRODUCTION

Fluid balance is a critical aspect of maintaining physiological stability, regulated through complex interactions between the kidneys and hormonal systems. For patients undergoing dialysis, particularly those with oligo-anuria, the kidneys lose their ability to effectively eliminate excess body fluids, leading to a consistently positive daily fluid balance. Estimating the amount of excess fluid to be removed during each hemodialysis session is an essential but challenging task, typically based on the patient's weight gain between dialysis sessions and clinical assessment [1]. Moreover, dry weight (the lowest tolerable post-dialysis weight) is difficult to measure precisely. The estimation is largely empirical, prone to error, and varies over time due to changes in a patient's health status, contributing to inaccuracies in managing fluid overload [2].

Fluid overload is considered as the most common and concerning risk factor in hemodialysis [3], significantly contributing to both short- and long-term morbidity [4]. Clinical assessment of fluid volume is often inadequate because patient symptoms—such as edema, dyspnea, or crackles—tend to manifest late, even when significant lung congestion is present [5]. Moreover, hypertension, often used as a marker

for fluid overload, is multifactorial in dialysis patients, further complicating accurate assessments [6].

Several methods have been proposed for dry weight assessment; unfortunately, these methods suffer from several shortcomings, such as poor specificity, operator dependence, and delayed correlation with extra cellular volume [7], [8]. Therefore, more accurate and objective methods are urgently needed to guide fluid management in these patients.

Recent advances suggest that lung ultrasound (LUS) is a promising tool for assessing fluid overload as it is more sensitive and equally specific compared to conventional chest X-rays [9]. LUS offers a non-invasive, objective, and potentially more accurate method for guiding fluid management in dialysis patients [7], [10]. However, despite these advancements, determining the optimal fluid status remains a challenge, often requiring a combination of clinical and technical parameters to improve precision and patient outcomes.

Deep learning techniques have enabled the use of multimodal models that integrate different types of medical data to improve predictive performance. Medical datasets often contain a wealth of clinical information in tabular form alongside imaging data, which poses both opportunities and challenges for model development. In clinical practice, however, medical datasets tend to be limited in scale and diversity, making deep learning models harder to train effectively. This has driven the development of methods that can pretrain multimodally, allowing for the use of unsupervised learning techniques to improve performance, especially when labeled data is scarce. Recent works have applied multimodal learning to various healthcare problems, such as contrastive learning frameworks [11] that combine images and tabular data to train unimodal encoders predicting risks of myocardial infarction and coronary artery disease [12], models that use tabular attention mechanisms to predict disease outcomes like Alzheimer's [13], and neural network that combines textual and tabular data to predict clinical deterioration in COVID-19 patients [14].

Despite advances in multimodal learning, no model has yet been proposed for predicting fluid overload in dialysis patients. This paper addresses that gap by integrating visual features from LUS images with clinical data. We extract tabular fea-

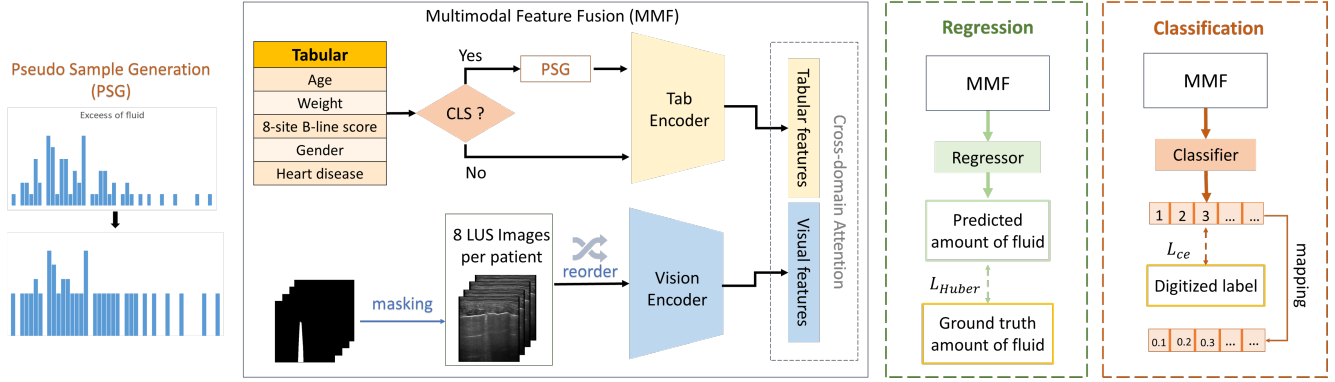


Fig. 1. A multimodal model framework for fluid overload prediction. “CLS” in the multimodal feature fusion module refers to classification. Pseudo sample generation is only implemented in the classification tasks.

tures and visual features using Multilayer Perceptron (MLP) and ResNet-50, respectively. The useful information is then merged via cross-domain attention. Although the goal is to estimate the amount of fluid which is a regression problem, merging two different types of data may produce high-entropy feature representations, and this is shown to be challenging for regression [15]. Therefore we treat the excess fluid prediction as a classification task to reduce the complexity of learning. Our experiments show more than 30% improvement of using multimodal data compared to the unimodal one. The study’s findings align with clinical needs for more reliable methods of managing fluid balance in dialysis patients.

II. METHODOLOGY

The proposed multimodal framework is shown in Fig. 1, comprising three components: pseudo sample generation, multimodal feature fusion, and classifier as regressor.

A. Pseudo sample generation

The distribution of the fluid overload suffers from significant class imbalances. Most patients fall within a narrow range of fluid overload values, while a smaller portion of patients exhibit extreme levels of under- or overhydration. This imbalance poses challenges for model training, as the model may become biased toward the majority class, leading to poor generalization of minority classes. To address this, we applied pseudo sample generation to augment the data, ensuring that all fluid overload classes are adequately represented in each mini-batch during training.

For a given sample x , consisting of continuous and categorical features, the function generates augmented samples \hat{x} by creating small random perturbations to the feature values. Let the continuous feature vector be x_{cont} and the categorical feature be x_{cat} . The augmented continuous features \hat{x}_{cont} are given by:

$$\hat{x}_{cont} = x_{cont} + \epsilon, \quad \epsilon \in \mathcal{N}(0, \sigma^2) \quad (1)$$

where ϵ is Gaussian noise with zero mean and standard deviation σ . The variation should be small enough to ensure that the new points are realistic and fall within the same class.

The categorical features are randomly perturbed with a probability of 50%. It is either left unchanged or replaced by a randomly selected value from the dataset:

$$\hat{x}_{cat} = \begin{cases} x_{cat}, & \text{probability 0.5} \\ \text{random_choice}(x_{cat} \in \text{dataset}), & \text{probability 0.5} \end{cases} \quad (2)$$

The final augmented sample \hat{x}_i is a combination of perturbed continuous features and potentially modified categorical features

$$\hat{x}_{cont} = [\hat{x}_{cont}, \hat{x}_{cat}] \quad (3)$$

This step increases the number of samples in the minority class and balances data distribution.

B. Multimodal Feature Fusion

Feature extraction: The model processes each data type through distinct feature extraction networks. The tabular data, which includes patient-specific attributes, is processed using a simple 2-layer MLP. This lightweight architecture is sufficient to extract relevant information from these clinical features, producing a vector of tabular features. For the LUS images, a deeper and more complex ResNet-50 architecture is employed to process the visual input, since LUS images contain rich patterns that correspond to fluid accumulation in the lungs. For this visual feature extraction, we input multiple LUS images per patient. This is because fluid overload often does not present in specific regions. For instance, fluid buildup might be more pronounced in the posterior regions due to gravity. Therefore, multiple LUS images will allow for a more comprehensive assessment of a patient’s condition, with each image representing a different imaging site.

In addition, LUS images contain some non-useful information that might confuse the network, especially muscles and tissue above plural lines. We therefore integrate the estimated mask to inform the useful areas in the LUS images to the network.

Cross-domain attention: Once the features are extracted from both tabular and visual data, a cross-domain attention mechanism is used to integrate these two data streams. This

allows the model to assign different levels of importance to each feature type, adapting its focus based on the specific context of the input data.

Given the two feature sets tabular features \mathbf{T} and visual features \mathbf{V} , the cross-domain attention mechanism applies scalar attention weights to each domain's features before they are combined for final prediction. Let α_T and α_V represents the importance of tabular and visual features respectively, the general equation for the cross-domain attention mechanism can be described as

$$\mathbf{F}_{combined} = \alpha_T \mathbf{T} + \alpha_V \mathbf{V}, \quad \alpha_T + \alpha_V = 1 \quad (4)$$

where $\mathbf{F}_{combined}$ is the combined feature vector after cross-domain attention. In the attention module, the softmax operation ensures the weights are non-negative and sum to 1.

The combined features are then fed into a classifier (or a regressor), a 2-layer MLP, that produces the final prediction of fluid overload.

C. Regression as classification

In the baseline model (see dashed green box in Fig. 1), a regressor is employed to predict fluid overload as a continuous variable, aiming to estimate the precise amount of excess fluid. However, this method can be challenging due to the inherent difficulty in learning exact fluid volumes from noisy and imbalanced data.

In computer vision, it is often observed that formulating regression problems as a classification task yields better performance [15]. A simple and common way is to discretize the continuous labels; each bin is then treated as a class. In this study, we adopt a similar approach for fluid overload prediction, where the amount of excess fluid is discretized into a predefined number of bins.

Let y_{true} represent the true continuous value of fluid overload for a given patient, $B = \{b_1, b_2, \dots, b_K\}$ represents the set of K bins, where each bin b_k corresponds to a range of fluid overload values:

$$b_k = \{[a_k, a_{k+1}) \mid a_k < a_{k+1}, k = 1, 2, \dots, K\} \quad (5)$$

The continuous label y_{true} is assigned to one of these bins, such that:

$$y_{class} = \text{argmax} \{b_k \mid y_{true} \in [a_k, a_{k+1})\} \quad (6)$$

Thus, the prediction task becomes a classification problem where the model predicts the most likely bin \hat{y}_{class} . In our case, the bins are carefully chosen to reflect clinically significant thresholds in fluid overload, balancing between granularity and the number of classes.

Once the model predicts the class \hat{y}_{class} , this can be mapped back to a representative continuous value r_k , which could be the midpoint of the bin or any other clinically meaningful value within the range.

III. IMPLEMENTATION DETAILS

A. Dataset

Data Collection and Preprocessing. The dataset used for this study was obtained from 65 patients at the Nephrology, Dialysis, and Transplantation Department of Careggi University Hospital in Florence, Italy. LUS evaluations were performed during the patients' regular hemodialysis sessions using an ultrasound machine (MyLab Class C-Esaote®, Genoa, Italy) with a 6–18 MHz linear probe. The collected data includes 8-site LUS videos for each patient along with the corresponding clinical records. The tabular records contain Patient ID, Collection Date, Gender, Age, Weight (kg), Dry Weight (kg), Excess Fluid (kg), Excess Fluid Percentage, 8-site B-line Score, and the Severity of Heart Disease. For each patient, the LUS image with the highest number of B-lines at each site was also extracted, as these images were used to calculate the B-line score, a sum of the maximum number of B-lines across all 8 lung sites.

Tabular Data Processing. Tabular feature selection was performed to eliminate irrelevant information, retaining only five independent features: Gender, Age, Weight, Excess Fluid (kg), 8-site B-line Score, and Severity of Heart Disease. Categorical features including Gender and Severity of Heart Disease, were one-hot encoded, while continuous features were normalized to the [0,1] range. In the classification tasks, pseudo samples were generated to make sure there are at least three samples in each class. The bin width for discretizing continuous labels was set to 0.1, striking a balance between granularity and the number of categories. During augmentation, consistency between the tabular and image data was maintained by augmenting only the tabular features excluding the 8-site B-line Score, which had to remain consistent with the corresponding LUS images. For each augmented sample, the nearest neighbor from the original data was used to determine the corresponding visual input.

Image Data Processing. LUS images were preprocessed by cropping the images to remove regions containing device information or imaging parameters and resizing them to 256×256 pixels. During training, a random reordering of the 8 images was applied, along with standard augmentations such as random horizontal flips and color jittering to increase model robustness. Additionally, B-line masks for each image were generated using a B-line detection model [16]. These masks were applied to the input images using a weighted sum to emphasize B-line regions.

B. Experimental Setup

We used the regression architecture as the baseline, where regressor is trained end-to-end using Huberloss to directly minimize the error between the predicted and actual fluid overload values. The loss function used for training the classification model is the cross-entropy loss, which measures the discrepancy between the predicted class probabilities and the true class label.

Five-fold cross-validation was used to evaluate the model's performance, and each fold was run five times, with each run

TABLE I
COMPARISON OF MULTIMODAL MODELS FOR FLUID OVERLOAD PREDICTION*

Experiment ID	1	2	3	4	5	6	7	8	9	10	11	12	13	14	15	16	17	18(ours)
Task Type	Regression																	
Modality	Classification																	
Attention Strategy**	Multimodal																	
Resample	Tabular																	
Pretraining Method	Visual																	
Loss Function	0.95/0.05																	
Mean Accuracy(%)	43.69	37.85	38.77	36.31	36.92	43.38	41.54	40.92	46.15	41.23	55.38	47.69	24.62	80.92	87.08	85.23	87.69	88.31
STD (%)	2.09	6.2	2.65	2.85	5.84	1.79	3.51	2.5	1.95	4.61	4.67	4.67	2.18	2.3	3.31	3.59	2.18	3.17

**": the setting is not applicable or not implemented; "I": ImageNet; "B": B-line detection work [16];

***": attention weight applied to the features $(num_1 \times \text{tabular feature}) / (num_2 \times \text{visual feature})$.

lasting 50 epochs. The results are the average of these five runs. The experiments compared the model performance on regression and classification tasks, different data modalities (tabular, visual, and multimodal), and the use of cross-domain attention mechanisms and data resampling techniques. We also investigated the performance of using pretrained visual encoders.

Model performance was evaluated according to clinical guidelines, where accuracy was considered acceptable if the prediction error for individual patients was within 0.5 kg [17], [18].

IV. RESULTS

Table I presents the results of ten regression-based experiments and eight experiments focused on classification tasks for predicting fluid overload. The experiments vary based on the modality (tabular, visual, or multimodal), attention strategies, data augmentation with pseudo sample generation, and pretraining methods.

It can be found that classification generally eases the learning process especially when tabular information is introduced. Our framework achieves an accuracy of 88.31%, which is significantly higher than the accuracies seen in the regression models. Additionally, most of the multimodal classification models (Experiments 14–18) achieved accuracies between 80.92% and 88.31%, showcasing the effectiveness of classification over regression.

In both classification and regression, the multimodal models consistently outperform single-modality models, demonstrating the effectiveness of combining tabular and visual features. Particularly, classification models benefit more from combining tabular and visual data. For single-modality models, the tabular-only model (Experiment 11) achieves 55.38% accuracy, which is the highest among the single-modality experiments. This indicates that tabular data alone carries substantial predictive power for fluid overload. The visual-only model (Experiment 13) achieves the lowest accuracy in the table, 24.62%, showing that LUS images alone are not sufficient to predict fluid overload. This highlights the complexity of interpreting LUS images in isolation. A similar trend is observed in the regression experiments: placing more attention on tabular features (0.95/0.05) results in better performance, indicating that clinical data (tabular) holds more

predictive power than visual data. Once supported by the right information from visual data, the accuracy of fluid estimation increases significantly.

The benefit of pseudo-sample generation is more pronounced in multimodal models. Our results shows clear benefits of pseudo-sample generation, significantly improving accuracy from 80.92% (Experiment 14) to 88.31%. However, in the tabular-only model (Experiment 12), pseudo-sampling reduced accuracy. This may be because the diversity of multiple data types allows the model to better handle and integrate synthetic data, leading to improved generalization. In contrast, tabular-only models lack this cross-modal validation and flexibility, leading to reduced performance when pseudo-sample generation is applied.

Pretraining is shown to be useful in regression, improving regression accuracy to 46.15% (Experiment 9), the best among regression models. Whereas in classification, though pertaining experiments show an accuracy over 85%, it is not as beneficial as that in regression.

We additionally tested both the CLIP [11] and Swin Transformer [19] models on the task of fluid overload prediction, but neither model showed notable improvements over the baseline methods, so we didn't list the result in the paper. The possible reason can be that the limited size of the medical dataset used in this study may have restricted their ability to learn effectively.

V. CONCLUSION

This paper presents a novel multimodal framework, where patient-specific attributes are integrate with LUS images, to predict their fluid overload. We proposed three components to deal with this useful but challenging data: i) pseudo sample generation to deal with highly imbalanced data; ii) multimodal feature fusion to merge useful information from two modalities; and iii) regression as classification to reduce learning complexity. The results show that the proposed framework can achieve 88.31% accuracy with more than 40% improvement over the baseline. Future work could expand these findings by leveraging larger, more diverse datasets to improve generalization and reduce the reliance on data augmentation techniques.

ACKNOWLEDGEMENT

This work has been submitted to the IEEE for possible publication. Copyright may be transferred without notice, after

which this version may no longer be accessible.

REFERENCES

- [1] J. T. Daugirdas, T. A. Depner, J. Inrig, R. Mehrotra, M. V. Rocco, R. S. Suri, D. E. Weiner, N. Greer, A. Ishani, R. MacDonald *et al.*, “KDOQI clinical practice guideline for hemodialysis adequacy: 2015 update,” *American journal of kidney diseases*, vol. 66, no. 5, pp. 884–930, 2015.
- [2] Y. Chait, G. Derk, D. Forfang, J. Flythe, N. Gooch, C. Herzog *et al.*, “Fostering innovation in fluid management,” *Kidney Health Initiative, Tech. Rep.*, 2019.
- [3] R. Agarwal, “Volume overload in dialysis: the elephant in the room, no one can see,” *American journal of nephrology*, vol. 38, no. 1, pp. 75–77, 2013.
- [4] M. J. Dekker and J. P. Kooman, “Fluid status assessment in hemodialysis patients and the association with outcome: review of recent literature,” *Current opinion in nephrology and hypertension*, vol. 27, no. 3, pp. 188–193, 2018.
- [5] C.-J. Wallin, S. Jacobson, and L. Leksell, “Subclinical pulmonary oedema and intermittent haemodialysis,” *Nephrology dialysis transplantation*, vol. 11, no. 11, pp. 2269–2275, 1996.
- [6] C. Chazot, P. Wabel, P. Chamney, U. Moissl, S. Wieskotten, and V. Wizemann, “Importance of normohydration for the long-term survival of haemodialysis patients,” *Nephrology Dialysis Transplantation*, vol. 27, no. 6, pp. 2404–2410, 2012.
- [7] C. Ekinici, M. Karabork, D. Siriopol, N. Dincer, A. Covic, and M. Kanbay, “Effects of volume overload and current techniques for the assessment of fluid status in patients with renal disease,” *Blood Purification*, vol. 46, no. 1, pp. 34–47, 2018.
- [8] B. Canaud, C. Chazot, J. Koomans, and A. Collins, “Fluid and hemodynamic management in hemodialysis patients: challenges and opportunities,” *Brazilian Journal of Nephrology*, vol. 41, no. 4, p. 550–559, Oct 2019. [Online]. Available: <https://doi.org/10.1590/2175-8239-JBN-2019-0135>
- [9] A. M. Maw, A. Hassanin, P. M. Ho, M. D. McInnes, A. Moss, E. Juarez-Colunga, N. J. Soni, M. H. Miglioranza, E. Platz, K. DeSanto *et al.*, “Diagnostic accuracy of point-of-care lung ultrasonography and chest radiography in adults with symptoms suggestive of acute decompensated heart failure: a systematic review and meta-analysis,” *JAMA network open*, vol. 2, no. 3, pp. e190703–e190703, 2019.
- [10] C. Zoccali, C. Torino, R. Tripepi, G. Tripepi, G. D’Arrigo, M. Postorino, L. Gargani, R. Sicari, E. Picano, F. Mallamaci *et al.*, “Pulmonary congestion predicts cardiac events and mortality in ESRD,” *Journal of the American Society of Nephrology*, vol. 24, no. 4, pp. 639–646, 2013.
- [11] A. Radford, J. W. Kim, C. Hallacy, A. Ramesh, G. Goh, S. Agarwal, G. Sastry, A. Askell, P. Mishkin, J. Clark *et al.*, “Learning transferable visual models from natural language supervision,” in *International conference on machine learning*. PMLR, 2021, pp. 8748–8763.
- [12] P. Hager, M. J. Menten, and D. Rueckert, “Best of both worlds: Multimodal contrastive learning with tabular and imaging data,” in *Proceedings of the IEEE/CVF Conference on Computer Vision and Pattern Recognition*, 2023, pp. 23924–23935.
- [13] W. Huang, “Multimodal contrastive learning and tabular attention for automated Alzheimer’s disease prediction,” in *Proceedings of the IEEE/CVF International Conference on Computer Vision*, 2023, pp. 2473–2482.
- [14] F. Dipaola, M. Gatti, A. Gajaj Levra, R. Menè, D. Shiffer, R. Faccincani, Z. Raouf, A. Secchi, P. Rovere Querini, A. Voza *et al.*, “Multimodal deep learning for COVID-19 prognosis prediction in the emergency department: a bi-centric study,” *Scientific Reports*, vol. 13, no. 1, p. 10868, 2023.
- [15] S. Zhang, L. Yang, M. B. Mi, X. Zheng, and A. Yao, “Improving deep regression with ordinal entropy,” *arXiv preprint arXiv:2301.08915*, 2023.
- [16] T. Yang, N. Anantrasirichai, O. Karakuş, M. Allinovi, and A. Achim, “A semi-supervised learning approach for B-line detection in lung ultrasound images,” in *2023 IEEE 20th International Symposium on Biomedical Imaging (ISBI)*. IEEE, 2023, pp. 1–5.
- [17] J. Schotman, N. Rolleman, M. van Borren, J. Wetzel, H. Kloke, L. Reichert, and H. de Boer, “Accuracy of bioimpedance spectroscopy in the detection of hydration changes in patients on hemodialysis,” *Journal of Renal Nutrition*, vol. 33, no. 1, pp. 193–200, 2023.
- [18] Y.-T. Shie, Y.-Y. Lai, and M.-H. Chin, “Reduce the body weight difference rate of hemodialysis patients,” in *29th International Nursing Research Congress*, Melbourne, Australia, July 2018.
- [19] Z. Liu, Y. Lin, Y. Cao, H. Hu, Y. Wei, Z. Zhang, S. Lin, and B. Guo, “Swin transformer: Hierarchical vision transformer using shifted windows,” in *Proceedings of the IEEE/CVF international conference on computer vision*, 2021, pp. 10012–10022.